NASA TECHNICAL NOTE

NASA TN D-2521

NASA TN D-2521

EXPERIMENTAL HEAT-TRANSFER AND BOUNDARY-LAYER BEHAVIOR WITH 100-CPS FLOW OSCILLATIONS

by Charles E. Feiler

Lewis Research Center

Cleveland, Ohio

NATIONAL AERONAUTICS AND SPACE ADMINISTRATION • WASHINGTON, D. C. • DECEMBER 1964

EXPERIMENTAL HEAT-TRANSFER AND BOUNDARY-LAYER BEHAVIOR WITH 100-CPS FLOW OSCILLATIONS

By Charles E. Feiler

Lewis Research Center
Cleveland, Ohio

NATIONAL AERONAUTICS AND SPACE ADMINISTRATION

For sale by the Office of Technical Services, Department of Commerce,
Washington, D.C. 20230 -- Price $1.00

EXPERIMENTAL HEAT-TRANSFER AND BOUNDARY-LAYER BEHAVIOR WITH 100-CPS FLOW OSCILLATIONS

by Charles E. Feiler

Lewis Research Center

SUMMARY

The time-averaged heat-transfer rates and velocity and temperature profiles on a cylinder in parallel subsonic airflow were measured in both steady and oscillating flows. In the steady reference flow, a laminar boundary layer and laminar heat transfer that agree with the Blasius relations were obtained for Reynolds numbers less than about 10^5. By addition of a boundary layer trip, transition to a turbulent layer was induced, transition having started at a Reynolds number of about 3×10^4. The data for the oscillating flow were compared with these two reference conditions. The results, without the boundary-layer trip, indicated that the effect of the oscillation was induced transition to turbulent flow. The only effect of the boundary-layer trip in oscillating flow was a further reduction in transition Reynolds number. The turbulent data, whether produced with the boundary-layer trip or with the oscillating flow, were in relatively good agreement with the universal logarithmic velocity and temperature profiles and with accepted turbulent heat-transfer relations.

INTRODUCTION

In a previous study of the effect of flow oscillations on the heat-transfer rate from a flat plate, it was found that the oscillations produced an increase in the heat-transfer rate (ref. 1). From this study it was uncertain whether the increase was a direct result of the oscillations or whether it was due to oscillation-induced transition from laminar to turbulent flow. The Reynolds number range of the experiment indicated the likelihood of transition flow, but the heat-transfer rates were somewhat higher than predicted values for turbulent flow even without oscillations. This result could have been a consequence of the 10-percent turbulence intensity of the flow. The present study was intended to resolve this question and to explore further the effects of flow oscillations.

The experiments were conducted on a cylindrical body in parallel flow instead of on a flat plate. The cylinder, because of its symmetry, is free of edge effects and heat-loss corrections, except in the axial direction. Also, if the diameter of the cylinder is not too small, it may be regarded as a flat plate. In addition to time-averaged heat-transfer coefficients, time-averaged velocity and temperature profiles of the boundary layer were measured. Both

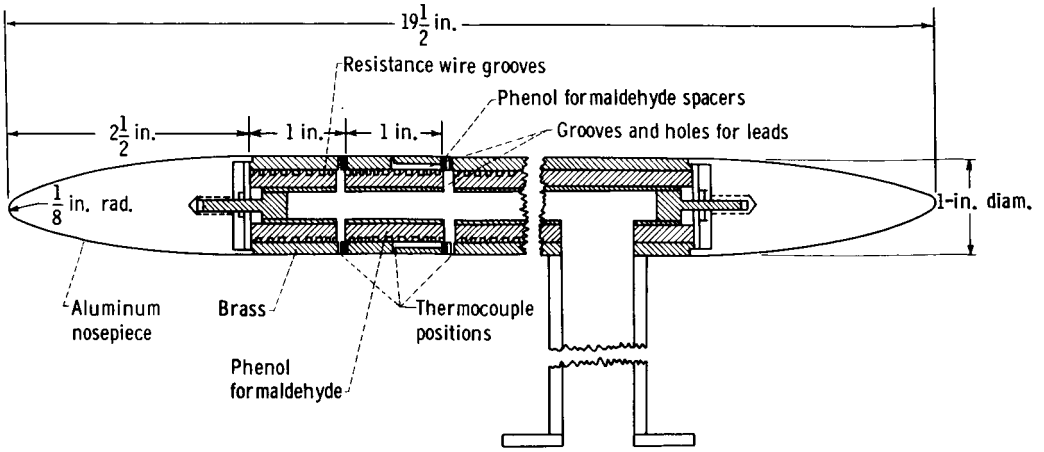

Figure 1. - Test cylinder.

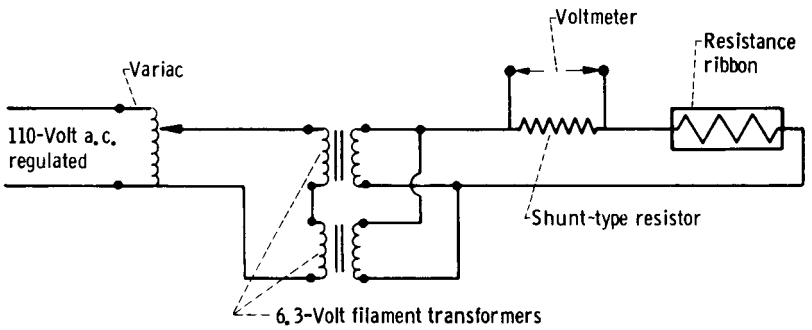

Figure 2. - Heater circuit.

laminar and turbulent boundary layers were studied, the latter being achieved in the reference flow by a boundary-layer trip.

The data were obtained at atmospheric pressure and temperature over a velocity range of about 15 to 150 feet per second corresponding to Reynolds numbers from about 10^4 to 10^5 based on axial length. The maximum temperature difference between the wall and the stream was about 60° F. The turbulence intensity of the reference flow was about 3 to 4 percent. A single oscillation frequency, produced by a siren, of 100 cps and about 50 percent root-mean-square amplitude was studied. (The previous study had indicated no independent effect of oscillation frequency, and it was not included as a variable.) Flow rates and velocity profiles were measured with a linearized constant-temperature hot-wire anemometer.

APPARATUS

Except for the test cylinder and some modification of the flow system, the apparatus was that described in reference 1. A cylindrical body was selected rather than a flat plate because of the absence of edge effects and lateral heat losses for which correction must be made. Theoretical studies of the cylinder in laminar flow (ref. 2) and in turbulent flow (ref. 3) indicate that for

the cylinder diameter and Reynolds numbers of the present experiment, deviations from flat-plate theory should be less than about 5 percent.

Test Cylinder

A diagram of the test cylinder is shown in figure 1. The brass outer shell had a 1-inch outside diameter with a 1/8-inch wall thickness. The nose piece and tailpiece were aluminum, shaped as illustrated, and unheated except by conduction. The main body was composed of three segments, insulated from each other by thin phenol formaldehyde washers and heated by separate resistance coils wound on an inner phenol formaldehyde core, which had a 3/16-inch wall thickness. The resistance wire was wound in helical grooves 0.05 inch deep that were then filled with a plastic material of good thermal conductivity but poor electrical conductivity. This inner heating core fit tightly into the brass tube and the whole assembly was held together under compression. The outer surface was polished to a mirror finish.

The front and rear heated sections were used as guard heater sections. Each had two 30-gage copper-constantan thermocouples located 180° apart and immediately adjacent to the center section. These couples were flush with the outer surface and in good thermal contact with, but electrically insulated from the brass. The center section, which was used for all heat-transfer measurements, was provided with four thermocouples at the midpoint and 90° apart. These four thermocouples were averaged in reducing the data. All thermocouples were referenced to a free-stream thermocouple by a multiposition switch so that temperature differences were read directly on a potentiometer.

A low-voltage alternating current was used to heat the resistance coils as shown in figure 2. The power dissipation in the coils was calculated from the measured current through the series resistor and the resistance of the coil. Resistances of the coils and series resistors were measured with a double Kelvin bridge to within 1 percent.

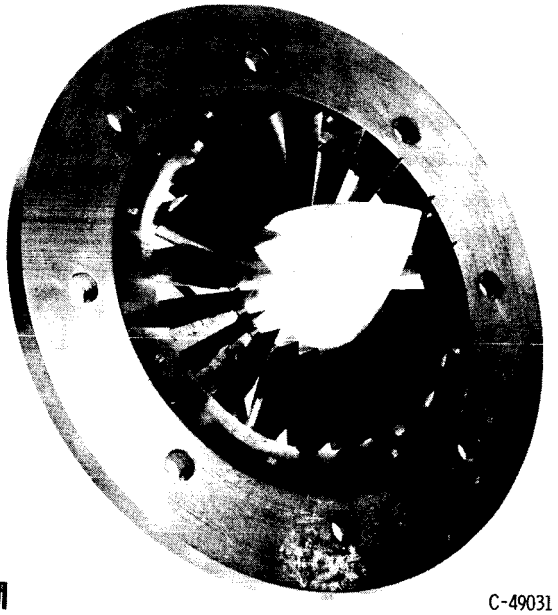

C-49031

Figure 3. - Siren assembly.

Flow System

A photograph of the siren is shown in figure 3. It has been described in reference 1. In the previous study, the siren was located at the inlet of the duct, and the eddy shedding that occurred resulted in a 10-percent turbulence intensity in the reference flow with the siren locked in the open position. Since it was thought that this turbulence intensity influenced the heat-transfer results, a means was sought to reduce it. This was accomplished by locating the siren downstream

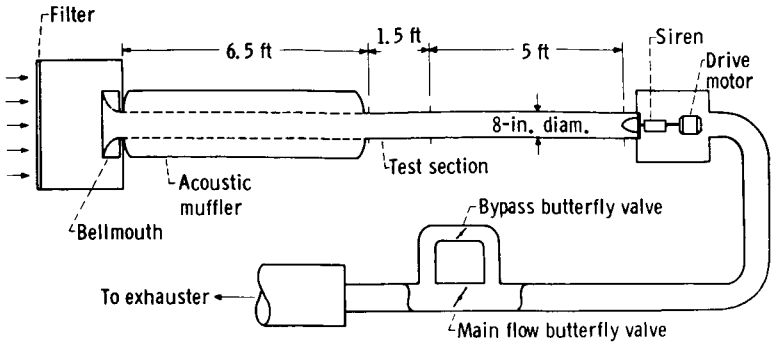

Figure 4. - Flow system.

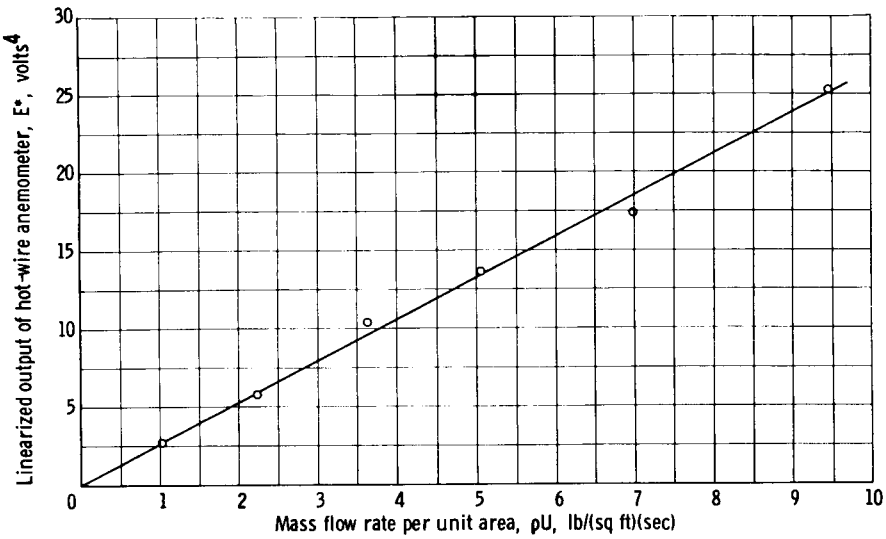

Figure 5. - Hot-wire calibration curve.

from the test section. The resulting flow system is shown in figure 4. The acoustic muffler, necessary to keep the external sound level at a reasonable value, was located upstream from the test section and was fitted with a bellmouth inlet. Air entering the duct was filtered through several layers of glass fiber mounted in the end of the enclosure around the inlet. With this system, the turbulence intensity of the reference flow was about 3 to 4 percent. Flow rates were controlled by the butterfly valves.

Instruments

A linearized hot-wire anemometer was used to measure the mean flow rates and velocity amplitudes. The equation for the output of the hot wire may be written

$$E^2 = E_o^2 + K\sqrt{\rho U} \tag{1}$$

so that the voltage function that is linear with flow rate is

$$E^* = (E^2 - E_o^2)^2 = K^2 \rho U \qquad (2)$$

where E_o is the voltage output without airflow. (All symbols are defined in the appendix.) The squaring operations were performed with commercially available analog computer modules, while the bucking voltage E_o^2 was generated with a battery and a potentiometer. In practice, the value of E_o^2 was established by adjusting the difference $E^2 - E_o^2$ to zero with no airflow. The average value and root-mean-square value of E^* were read on a direct-current electronic voltmeter and a true root-mean-square voltmeter, respectively. The hot wire was calibrated against a pitot-static tube for which the pressure head was read on a micromanometer. A typical calibration curve is shown in figure 5. The hot wires were tungsten, 0.0002 inch in diameter and 0.08 inch long.

For measuring temperature profiles, a thermocouple probe identical in geometry to the hot-wire probe was constructed. Chromel-constantan wires 0.001 inch in diameter were butt-welded under a microscope by electrical fusion. These materials, which have the highest sensitivity of any of the common thermocouple materials, were selected because of the relative ease with which the junction could be fabricated. Use of the procedure and nomographs of reference 4 showed the time constant of the thermocouple to be, at most, about 20 milliseconds, while the error in air temperature measurement due to conduction and radiation was negligible (<0.2 percent). This thermocouple was also referenced to a free-stream thermocouple of the same material.

In measuring velocity and temperature profiles, a continuous trace of the hot-wire or thermocouple signal was recorded on an X-Y plotter as the boundary layer was traversed. For this purpose the thermocouple signal was amplified 100 times. The linearized output of the hot wire did not require amplification.

Traversing Device

The probes were mounted in a motor-driven actuator for traversing the boundary layer. Continuous records of either velocity or temperature against position were obtained with an X-Y plotter. Position was indicated by the voltage across a 10-turn 1000-ohm potentiometer geared to the actuator mechanism. The system was calibrated against a dial indicator that could be read to 0.0001 inch. The sensitivity of the actuator system was about 2000 ohms per inch of probe travel. The rate of probe travel was about 0.1 inch per minute, a sufficient time to allow the X-Y plotter to average the instrument signals.

PROCEDURE AND REDUCTION OF DATA

As in the previous study, the reference flow was obtained with the siren ports locked in the fully open position. Heater voltages were adjusted to give approximately equal temperatures in the three sections. For each flow condition time was allowed to attain equilibrium and then power and temperature readings were taken for four 5-minute intervals.

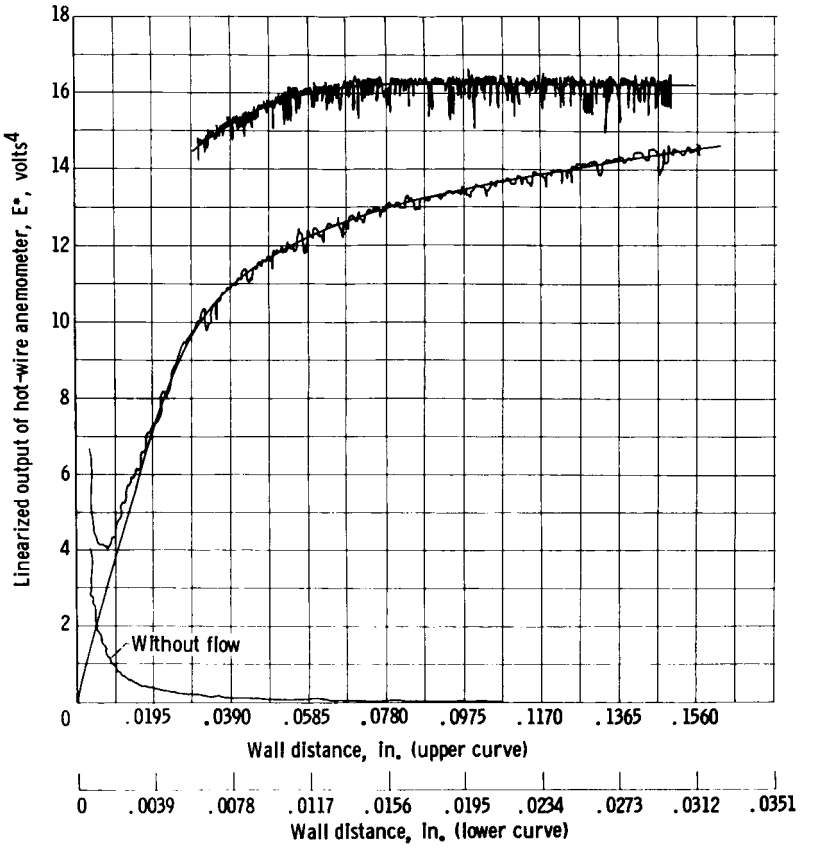

(a) Velocity.

Figure 6. - Typical surveys obtained with X-Y plotter.

Heat-transfer rates were measured from the center section only. The heat-transfer coefficient was calculated from the power input corrected for any axial heat conduction and the temperature difference between the surface and the air stream. The conduction exchange was calculated from the measured temperature difference between adjacent sections by assuming that the gradient occurred entirely across the insulating sections. This correction never exceeded about 5 percent of the input heat.

In obtaining the boundary-layer profiles, each time a traverse was made, the probe was first contacted with the test cylinder surface, as indicated by electrical continuity, and then moved away until continuity was just broken. This procedure served to establish the position of the probe with respect to the wall and also to eliminate any backlash in the gear train of the actuator. Initial alinement of the probe was accomplished while observing the sensing element of the probe and its image in the brass surface through a microscope.

Typical boundary-layer traverses as obtained on the X-Y plotter are shown in figure 6. A greatly expanded distance scale was employed for approximately the first 0.030 inch from the wall in order to obtain increased sensitivity. The fluctuations in the curves are due to fluctuations in the velocity or temperature field but are limited in range to the frequency response of the plot-

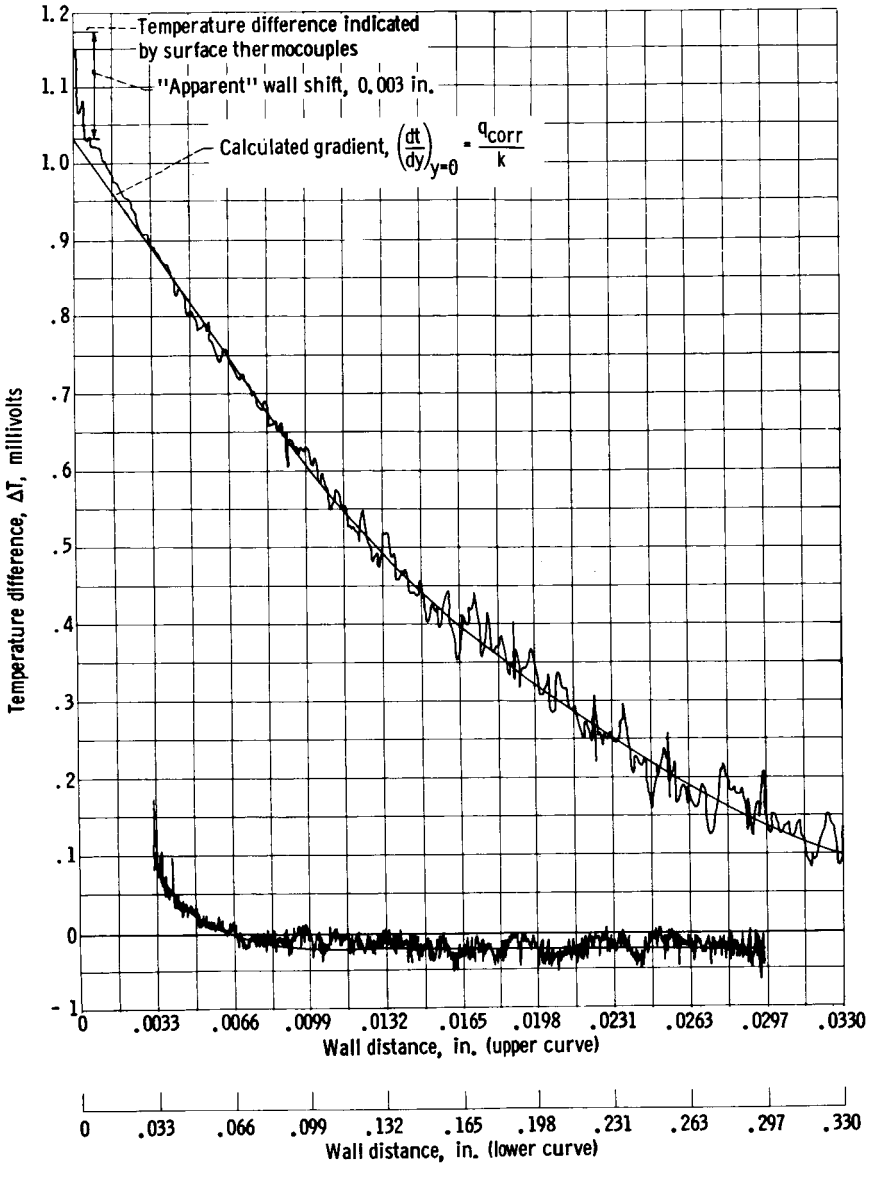

(b) Temperature.

Figure 6. - Concluded. Typical surveys obtained with X-Y plotter.

ter. Average curves were drawn as shown through these traces and the data points used to represent a profile are readings taken at regular intervals on these curves.

In the vicinity of the wall, the hot wire indicated a velocity even without airflow because of heat conduction to the wall. (The wire temperature was of the order of 300° F.) It was thus necessary to precede each profile measurement by a partial traverse without flow. This curve (see fig. 6(a)) was subtracted from the velocity profile to give a corrected profile. In general, the heat conduction correction became negligible at distances greater than 0.004 inch from the wall. In extrapolating the corrected profile to the wall, a linear slope and zero velocity at the wall were assumed.

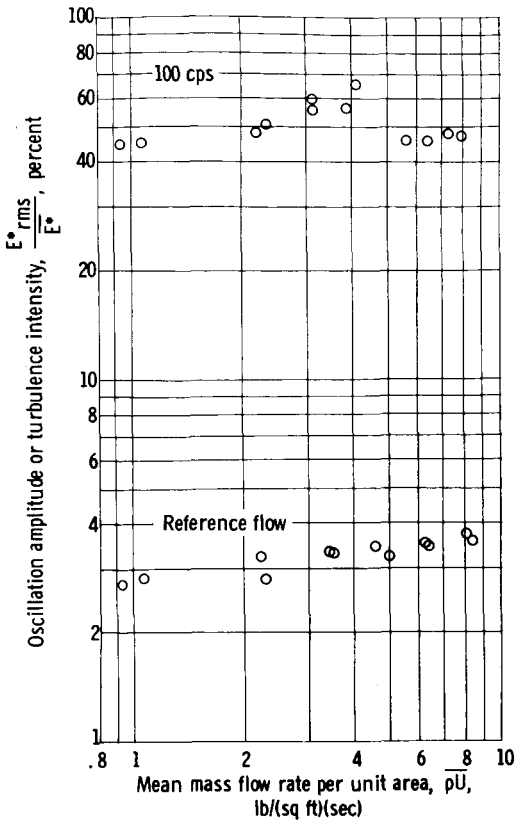

Figure 7. - Oscillation amplitude and turbulence intensity.

For the temperature profiles, the wall temperature was taken as that measured by the surface thermocouples. The gradient at the wall was assumed to be linear and was calculated from the experimental heat input corrected for axial conduction and the thermal conductivity of air at the wall temperature. This procedure resulted in an apparent shift in some of the profiles of as much as 0.003 inch, as shown in figure 6(b).

As will be shown subsequently, a laminar boundary-layer flow was obtained at the test section in the reference flow. In order to obtain a turbulent layer, a trip device consisting of a 0.02-inch-thick layer of masking tape was placed on the aluminum nosepiece. The tape extended 1/4 inch in the axial direction and terminated at the trailing edge of the nosepiece.

RESULTS AND DISCUSSION

The data obtained included heat-transfer rates and velocity and temperature profiles all of which were time-averaged. Since frequency was not shown to be an independent parameter in the previous study, only a single frequency of 100 cps was studied. This frequency was a resonant frequency of the duct. It should also be pointed out that the wavelength of the oscillation was greater than any characteristic dimension of the test cylinder or of the boundary layer. The root-mean-square oscillation amplitude is plotted in figure 7 against the time-averaged mass flow rate per unit area. Also shown is the turbulence tensity of the reference flow. These averaged about 50 and 3 percent, respectively. The oscillation amplitude was sufficiently large to produce a small reversal in free-stream flow. Flow reversal was also observed in the previous study and is described in reference 1. The reverse-flow region was averaged as a positive flow in determining the time-averaged flow rate.

As pointed out earlier, it should be possible to treat the cylinder as a flat plate; however, it might be expected that some correction would be needed to account for the shape of the leading edge, especially since measurements were made so near to the leading edge. This, in fact, proved to be true, and a correction was made in axial distance to give an equivalent flat-plate length. The correction was determined from consideration of the velocity profiles. In the reference flow, traverses of the boundary layer gave the result shown in figure 8, where the ratio of local velocity to free-stream velocity U/U_∞, is plotted against the Blasius parameter

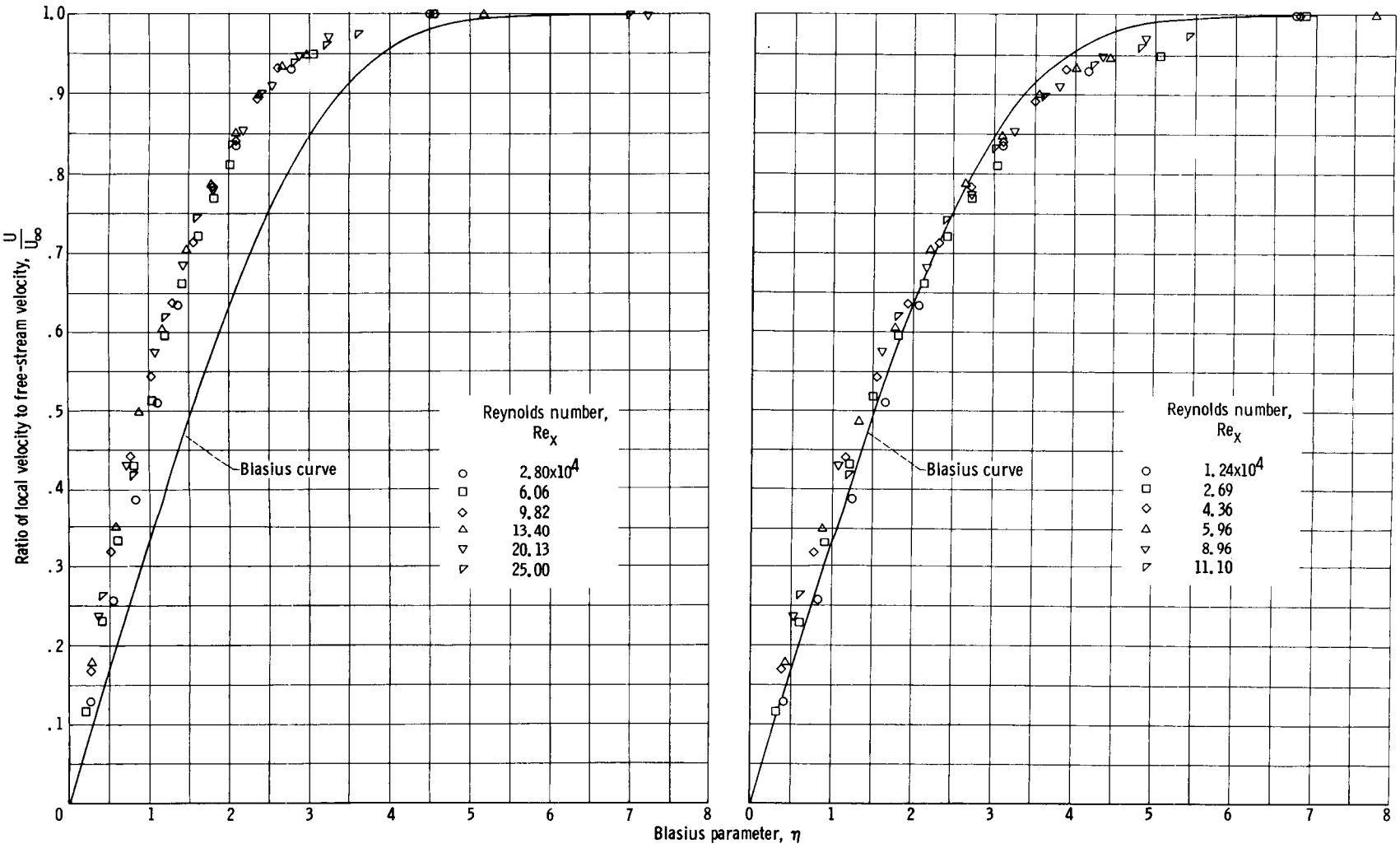

(a) Reynolds numbers and Blasius parameters computed by using actual x-distance.

(b) Reynolds numbers and Blasius parameters computed by using corrected x-distance.

Figure 8. - Velocity profiles for steady-state flow without boundary-layer trip.

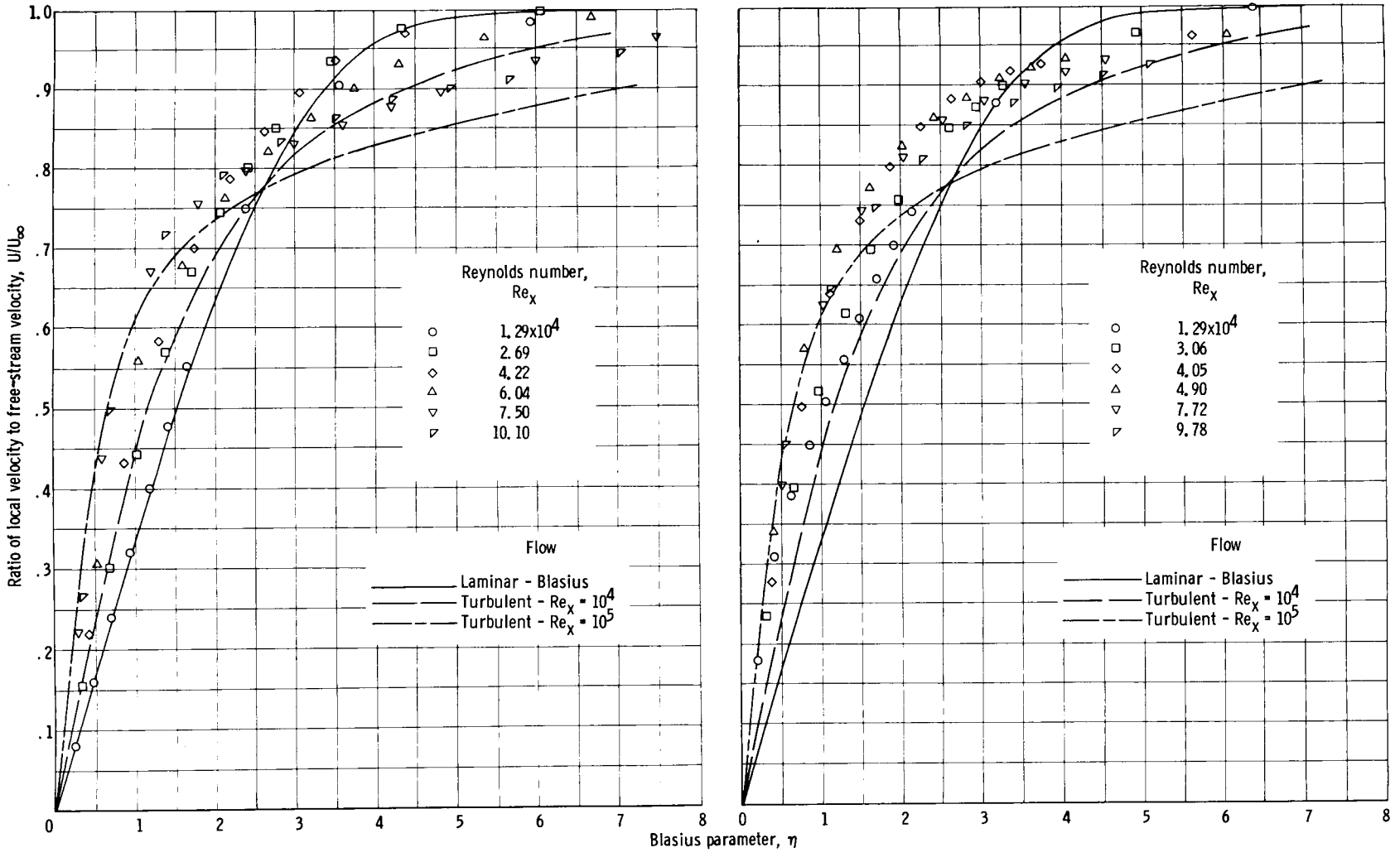

(a) Steady-state flow with boundary-layer trip.

(b) Oscillating flow without boundary-layer trip.

Figure 9. - Velocity profiles.

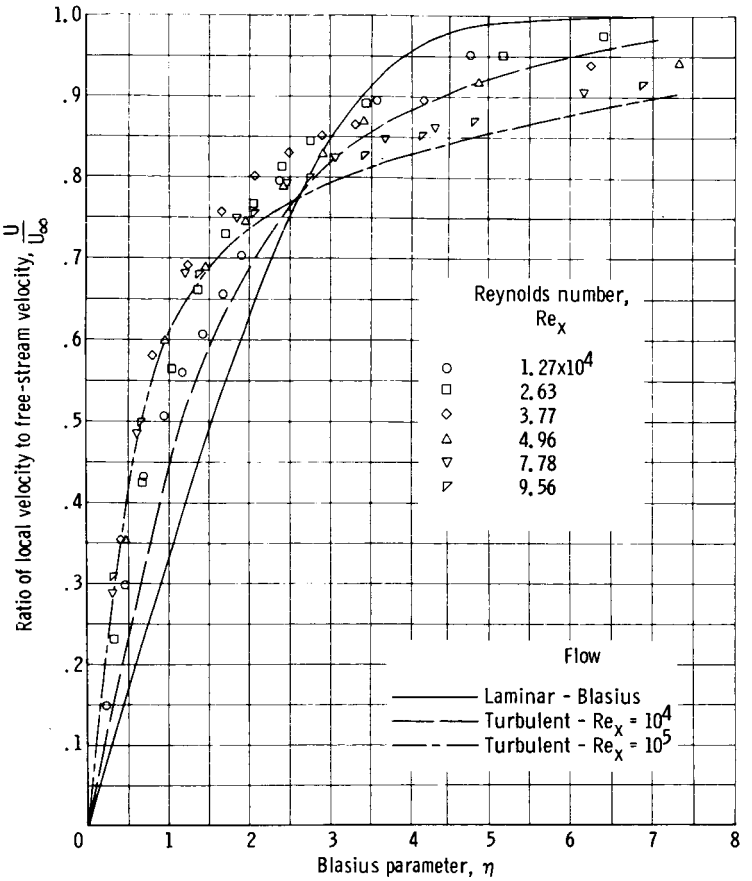

(c) Oscillating flow with boundary-layer trip.

Figure 9. - Concluded. Velocity profiles.

$$\eta = y \sqrt{\frac{\rho U_\infty}{\mu x}}$$

In figure 8(a), the data are shown with the actual axial distance from the leading edge (x = 4 in.) used in the computation of the Blasius parameter. It can be seen that the data approximate the Blasius curve but have a different slope. In figure 8(b), the data are shown plotted for x = 1.78 inches, which increases the experimental values of η by a factor of 1.5, since x appears to the negative one-half power. By adjustment of the x-length as shown, very good agreement was obtained with the Blasius profile. The effective x-length has been taken as 1.78 inches in all subsequent correlation and discussion.

In figure 9(a) are shown data obtained with the boundary-layer trip and in the reference flow. In addition to the Blasius curve, two turbulent profiles obtained from the "universal" profile relations are shown. At the lowest Reynolds number, the data agree with the Blasius profile. As the Reynolds number was increased, the profiles became steeper near the wall and flatter in the outer portions and generally appear to be similar to the turbulent profiles.

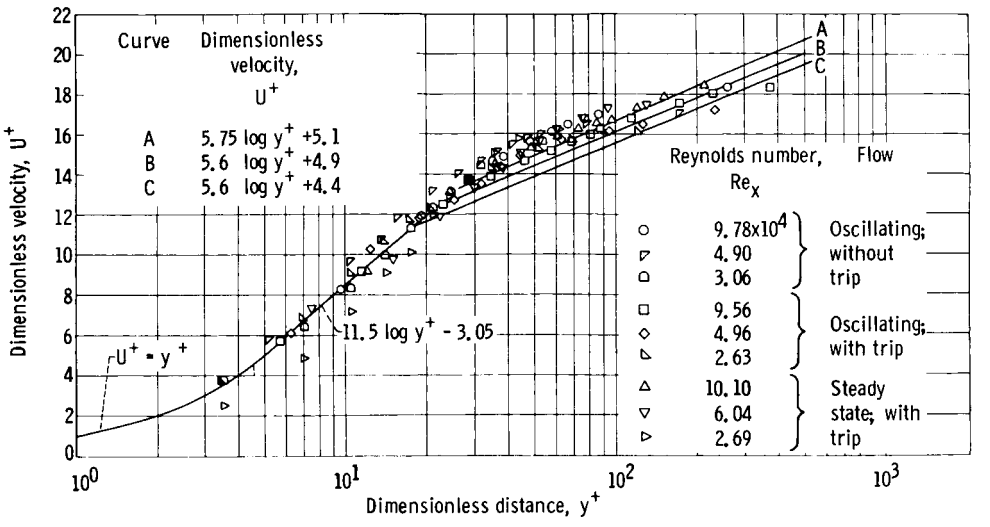

Figure 10. - Comparison of experimental velocity profiles with "universal" velocity profile.

Profiles in oscillating flow without and with the boundary-layer trip are shown in figures 9(b) and (c), respectively. These data do not follow the Blasius profile and resemble those obtained in the reference flow with the boundary-layer trip (fig. 9(a)).

One may inquire if the profiles that deviate from the laminar profile are representative of turbulent profiles. Turbulent profiles are usually represented by the universal profile in which the boundary layer is divided into three regions according to the viscous properties of each.

In the laminar sublayer adjacent to the wall $y^+ \leq 5$, the relation is

$$U^+ = y^+ \tag{3}$$

where

$$U^+ = \frac{U}{U_\infty} \frac{1}{\sqrt{\frac{C_f}{2}}}$$

and

$$y^+ = \frac{\rho U_\infty y}{\mu} \sqrt{\frac{C_f}{2}}$$

and C_f is the local coefficient of skin friction.

In the transition layer for $5 < y^+ < 26$ (ref. 5)

$$U^+ = 11.5 \log y^+ - 3.05 \tag{4}$$

and in the turbulent core for $y^+ > 26$

$$U^+ = a \log y^+ + b \tag{5}$$

where the values of a and b depend upon the investigator and have been variously determined as follows:

a	b	Source
5.6	4.4	Ref. 5
5.6	4.9	Ref. 6
5.75	5.1	Ref. 6

In order to compare the experimental profiles with the universal profile, the local coefficient of skin friction needed to normalize the data was computed, by using experimental values of the Reynolds number, according to the relation for a turbulent boundary layer (ref. 7)

$$\frac{C_f}{2} = 0.0296 \, Re_x^{-0.2} \tag{6}$$

The result is shown in figure 10, where U^+ is plotted against y^+. Also shown are the curves represented by the foregoing semiempirical relations. Within the spread of the data, there appears to be no distinction among the profiles that can be attributed to the flow conditions. One profile, that at the lowest Reynolds number of 2.69×10^4 in the reference flow, deviates from the others because it is much closer to laminar flow. While the experimental profiles do not agree perfectly with the literature curve, there appears to be sufficient similarity to warrant the conclusion that they are typical turbulent profiles. From the velocity profiles, the primary effect of flow oscillation appears to be the inducing of early transition to turbulent flow.

Figure 11 shows the temperature profiles in the same sequence of flow conditions shown for the velocity profiles. The temperature profiles are similar to the velocity profiles. For the reference flow with no trip, the data followed the Blasius curve when the x-length correction, previously discussed, was applied giving additional support to this correction.

A universal temperature profile was calculated for the turbulent boundary layer according to the assumptions and procedure of reference 5 and is presented in figure 12. The experimental profiles expressed in terms of a dimensionless temperature T^+ are also presented. Experimental values of T^+ are given by the definition

$$T^+ = \frac{\frac{C_f}{2}}{St} \frac{T_w - T}{T_w - T_\infty} \tag{7}$$

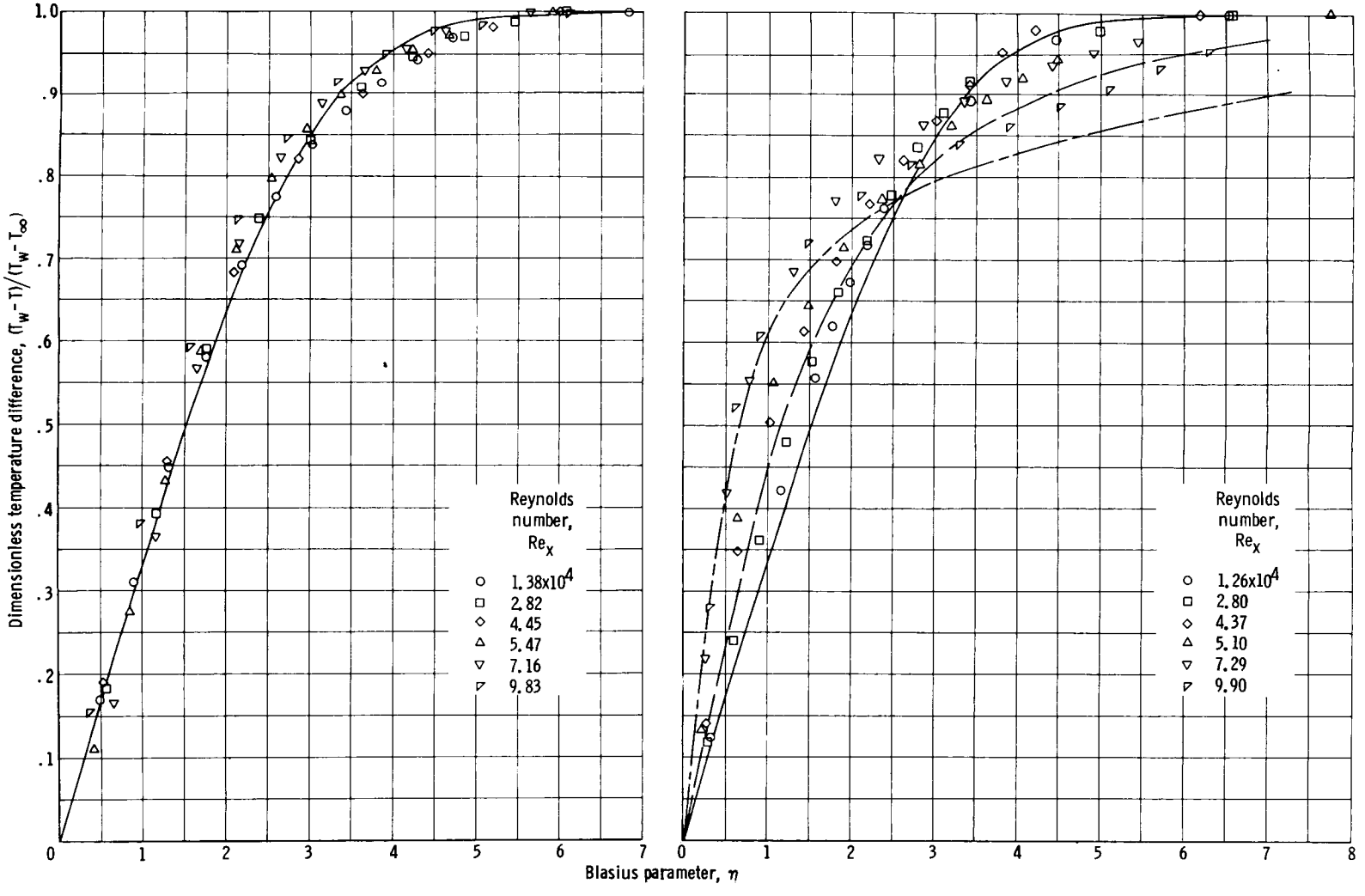

(a) Steady-state flow without boundary-layer trip.

(b) Steady-state flow with boundary-layer trip.

Figure 11. - Temperature profiles.

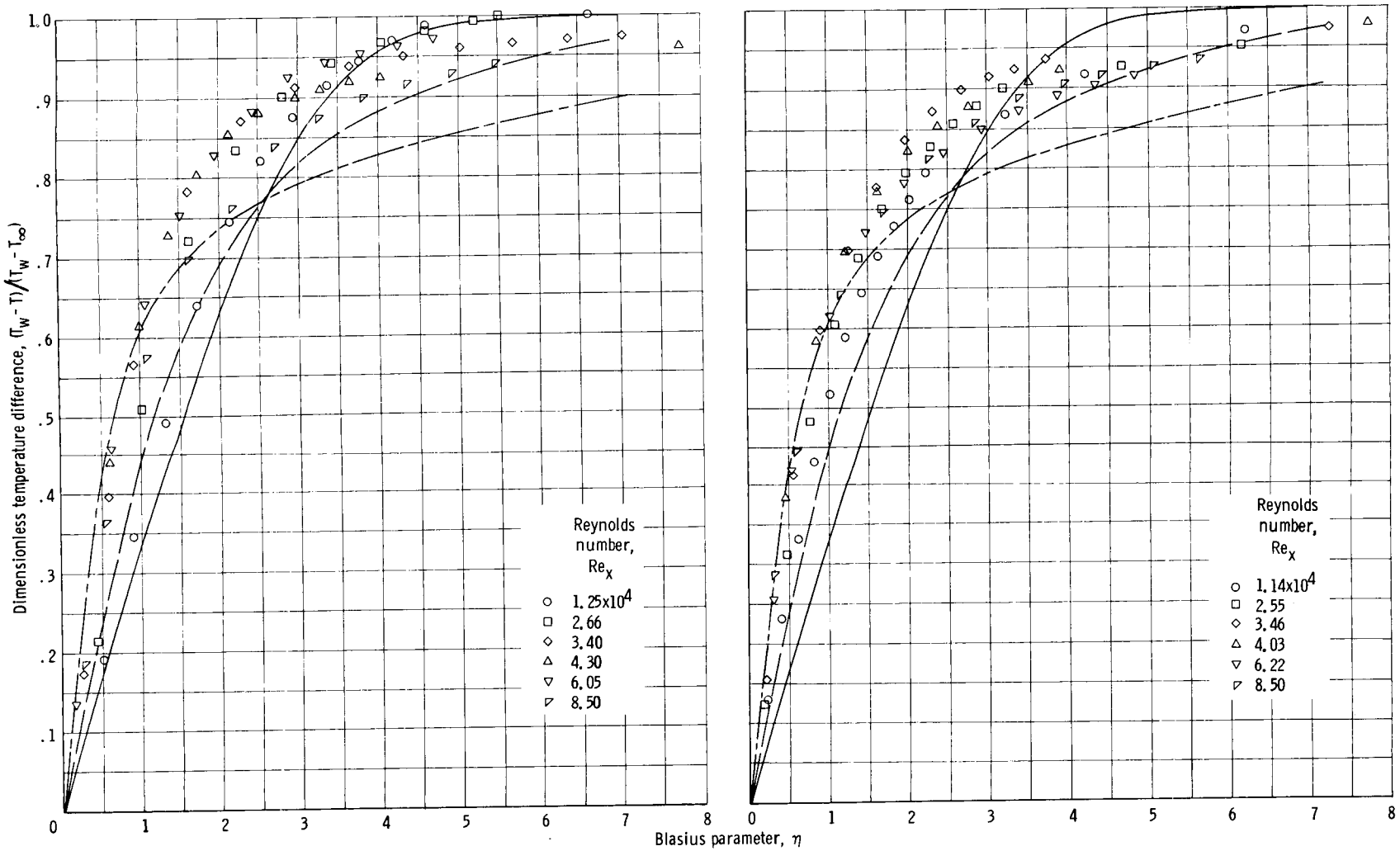

(c) Oscillating flow without boundary-layer trip.

(d) Oscillating flow with boundary-layer trip.

Figure 11. - Concluded. Temperature profiles.

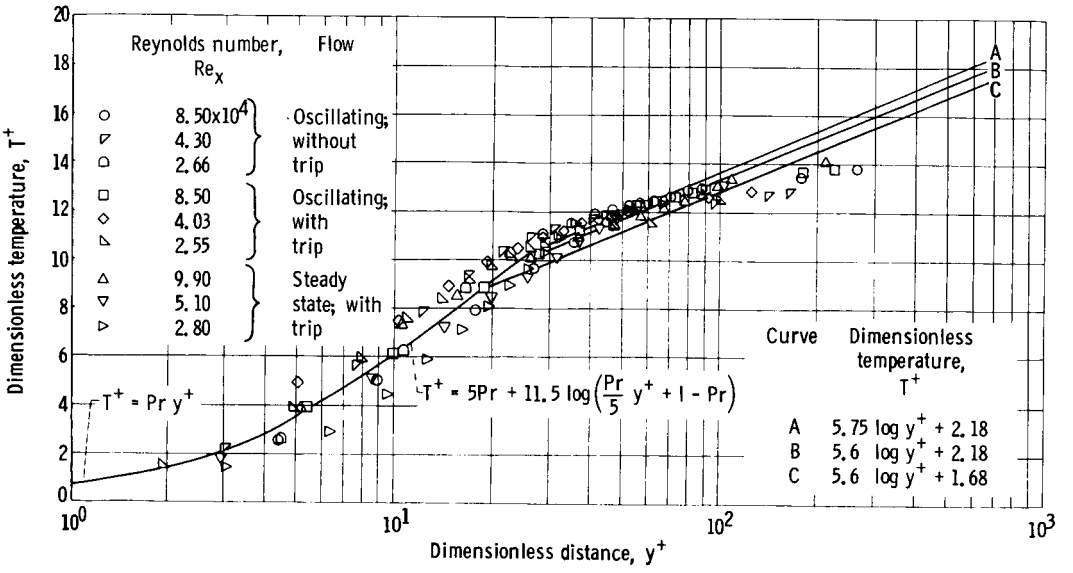

Figure 12. - Comparison of experimental temperature profiles with universal temperature profile.

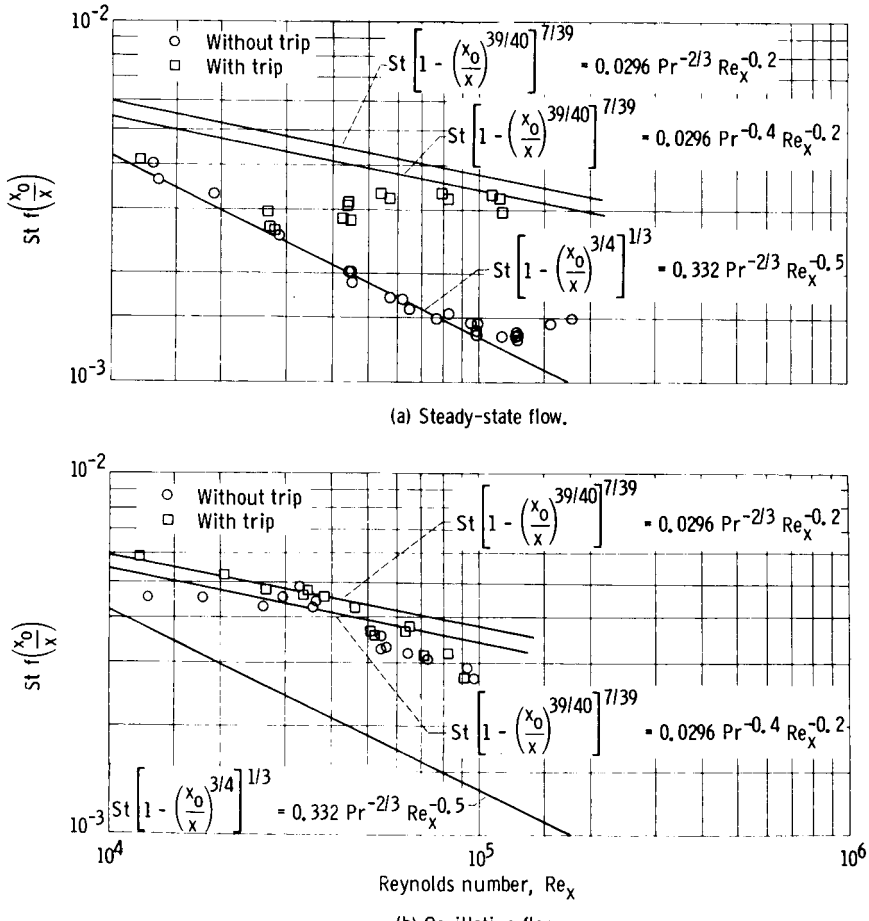

(a) Steady-state flow.

(b) Oscillating flow.

Figure 13. - Heat-transfer data.

where skin friction was calculated from the relation previously given (eq. (6)) and the Stanton number was calculated from the relation

$$\left[1 - \left(\frac{x_o}{x}\right)^{39/40}\right]^{7/39} \quad St = 0.0296\ Pr^{-2/3}\ Re_x^{-0.2} \tag{8}$$

The results shown in figure 12 show relatively good agreement with the theoretical curve.

The heat-transfer results are shown in figure 13, where Stanton number is plotted against Reynolds number. For laminar heat transfer the Blasius relation given by

$$\left[1 - \left(\frac{x_o}{x}\right)^{3/4}\right]^{1/3} \quad St = 0.332\ Pr^{-2/3}\ Re_x^{-0.5} \tag{9}$$

is shown for comparison. For turbulent flow, the relation given previously (eq. (8)) and

$$\left[1 - \left(\frac{x_o}{x}\right)^{39/40}\right]^{7/39} \quad St = 0.0296\ Pr^{-0.4}\ Re_x^{-0.2} \tag{10}$$

are shown. For the unheated starting length factors, given in reference 8, x was taken as the corrected length derived from the velocity profiles and $x_o = x - x_{ht}$, where x_{ht} is the actual heated length up to the point of measurement. The turbulent factor was applied to all the data in oscillating flow and to those data at Reynolds numbers larger than 5×10^4 in the tripped steady-state flow. Numerically, the use of these factors amounted to reduction of the experimental Stanton numbers by 3 percent for the turbulent case and 9 percent for the laminar case.

Good agreement with the Blasius relation was found for the laminar heat-transfer data (fig. 13(a)). Without a boundary-layer trip, transition was observed to start in the reference flow at a Reynolds number of about 10^5. Addition of the trip caused transition to start at a Reynolds number of about 3×10^4. In the oscillating flow without the trip, transition appears to have started at a Reynolds number of about 10^4 (fig. 13(b)). With the trip, transition was complete at the lowest Reynolds number studied. The data do not agree with either curve exactly, falling below both curves at the higher Reynolds numbers; however, the data obtained with the trip agree with those obtained without the trip.

CONCLUDING REMARKS

From the three kins of data, heat transfer and velocity and temperature profiles, it appears that the effect of the flow oscillation was to produce transition to turbulent flow. The use of sound to produce transition has been

reported in the literature at least as early as 1948 (ref. 9). The profiles and heat-transfer data obtained in this study with flow oscillations could not be distinguished from those obtained in the reference flow with a boundary-layer trip. In this case the oscillations perhaps could be considered more effective than the particular boundary-layer trip used in inducing transition. In a recent study of the effect of localized sonic excitation of a laminar boundary layer it was also concluded that the essential effect was premature transition to turbulent flow (ref. 10). In another study the transition Reynolds number decreased with the amplitude of the flow oscillation while appearing to be independent of oscillation frequency (ref. 11).

Since the interest in flow oscillations stems largely from the effects observed in rocket chambers during combustion instability, one may speculate concerning the relation of these results to the increased heat transfer and chamber burnout occurring during combustion instability. Generally chamber burnout seems to occur on the injector face or in the vicinity of the injector where velocities are normally fairly small. The mode of the oscillation seems to be important because burnout occurs more with the transverse mode than with the longitudinal mode. In this circumstance, it seems likely that the transverse oscillation could produce a large increase in the average velocity at the injector thus increasing the heat-transfer rate, as well as changing the heat-transfer process from laminar or perhaps even free convection to turbulent. An increase of several times might be expected under such circumstances. The longitudinal mode has a velocity node at the injector and therefore causes little increase in heat transfer.

SUMMARY OF RESULTS

Heat-transfer coefficients and velocity and temperature profiles were measured on a cylinder in parallel flow in both a steady and an oscillating flow. A laminar boundary layer and laminar heat transfer were obtained in the steady flow. By the addition of a boundary-layer trip transition to turbulent flow was obtained. For the unsteady case, the oscillation frequency was 100 cps and the root-mean-square amplitude was about 50 percent of the mean flow rate. The results may be summarized as follows:

1. In the reference flow without oscillations and without boundary-layer trip, the Blasius relations for heat transfer and temperature and velocity profiles were in good agreement with the data.

2. Addition of a boundary-layer trip induced transition to turbulent flow with the data correlated by usual heat-transfer relations and the universal velocity and temperature profiles. Transition started at a Reynolds number, based on x-length, of about 3×10^4.

3. With flow oscillations, the data were in agreement with the theoretical turbulent heat-transfer relations and temperature and velocity profiles. Addition of the boundary-layer trip introduced no further changes except that the transition Reynolds number was further reduced.

4. The data from all three types of measurement support the conclusion that the increased heat-transfer coefficient with oscillations is caused by the induced transition from laminar to turbulent flow.

Lewis Research Center
National Aeronautics and Space Administration
Cleveland, Ohio, August 18, 1964

APPENDIX - SYMBOLS

C_f	skin friction
E	nonlinearized output of hot-wire anemometer, volts
E_o	nonlinearized output of hot-wire anemometer without airflow, volts
E^*	linearized output of hot-wire anemometer, $volts^4$
K	constant, $volts^2/[lb/(sq\ ft)(sec)]^{1/2}$
k	thermal conductivity, Btu/(hr)(ft)(^oF)
Pr	Prandtl number
q_{corr}	heat flux, Btu/(hr)(sq ft)
Re_x	Reynolds number
St	Stanton number
T	temperature, ^oF
T_w	wall temperature, ^oF
T^+	dimensionless temperature, $\frac{\sqrt{C_f/2}}{St} \frac{T_w - T}{T_w - T_\infty}$
U	velocity (x-direction), ft/sec
U^+	dimensionless velocity, $\frac{U}{U_\infty} \frac{1}{\sqrt{C_f/2}}$
x	distance along cylinder measured from effective leading edge, ft
x_{ht}	heated length along cylinder, ft
x_o	unheated starting length, ft
y	distance normal to cylinder surface, ft
y^+	dimensionless y-distance, $\frac{\rho U_\infty y}{\mu} \sqrt{C_f/2}$
η	Blasius parameter, $y\sqrt{\frac{\rho U_\infty}{\mu x}}$
μ	viscosity, lb/(ft)(sec)
ρ	density, lb/cu ft

Subscripts:

rms root mean square

∞ free stream

Superscript:

$\bar{(\ )}$ average value

REFERENCES

1. Feiler, Charles E., and Yeager, Ernest B.: Effect of Large-Amplitude Oscillations on Heat Transfer. NASA TR R-142, 1962.

2. Seban, R. A., and Bond, R.: Skin-Friction and Heat-Transfer Characteristics of a Laminar Boundary Layer on a Cylinder in Axial Incompressible Flow. Jour. Aero. Sci., vol. 18, no. 10, Oct. 1951, pp. 671-675.

3. Sparrow, E. M., Eckert, E. R. G., and Minkowycz, W. J.: Heat Transfer and Skin Friction for Turbulent Boundary Layer Flow Longitudinal to a Circular Cylinder. Jour. Appl. Mech., (ASME Trans.), ser. E, vol. 30, no. 1, Mar. 1963, pp. 37-44.

4. Scadron, Marvin D., and Warshawsky, Isidore: Experimental Determination of Time Constants and Nusselt Numbers for Bare-Wire Thermocouples in High-Velocity Air Streams and Analytic Approximation of Conduction and Radiation Errors. NACA TN 2599, 1952.

5. Reynolds, W. C., Kays, W. M., and Kline, S. J.: Heat Transfer in the Turbulent Incompressible Boundary Layer. I - Constant Wall Temperature. NACA MEMO 12-1-58W, 1958.

6. Schubauer, G. B., and Tchen, C. M.: Turbulent Flow. Vol. V of High Speed Aerodynamics and Jet Prop., C. C. Lin, ed., Princeton Univ. Press, 1959.

7. Schlichting, H.: Boundary Layer Theory. McGraw Hill Book Co., Inc., 1955.

8. Hartnett, J. P., Eckert, E. R. G., Birkebak, Roland, and Sampson, R. L.: Simplified Procedures for the Calculation of Heat Transfer to Surfaces with Non-Uniform Temperatures. TR 56-373, WADC, Dec. 1956.

9. Schubauer, G. B., and Skramstad, H. K.: Laminar-Boundary-Layer Oscillations and Transition on a Flat Plate. NACA Rep. 909, 1948.

10. Jackson, Francis J., and Heckl, Manfred A.: Effect of Localized Acoustic Excitation on the Stability of a Laminar Boundary Plane. ARL 62-362, Aero. Res. Lab., June 1962.

11. Miller, J. A., and Fejer, A. A.: Transition Phenomena in Oscillating Boundary-Layer Flows. Jour. Fluid Mech., vol. 18, pt. 3, Mar. 1964, pp. 438-448.

NASA-Langley, 1964 E-2690